International Journal of Medical Physics, Clinical Engineering and Radiation Oncology, 2019, 8, 68-79
http://www.scirp.org/journal/ijmpcero
ISSN Online: 2168-5444
ISSN Print: 2168-5436

Evaluation of Daily Tumor Motion by Measuring Fiducial Length on CBCT Images in Pancreatic Stereotactic Body Radiation Therapy

Si Young Jang*, Min-Sig Hwang, Ron Lalonde, Dwight E. Heron, M. Saiful Huq

Department of Radiation Oncology, UPMC Hillman Cancer Center, School of Medicine, University of Pittsburgh, Pittsburgh, PA, USA
Email: *jangs@upmc.edu

How to cite this paper: Jang, S.Y., Hwang, M.-S., Lalonde, R., Heron, D.E. and Huq, M.S. (2019) Evaluation of Daily Tumor Motion by Measuring Fiducial Length on CBCT Images in Pancreatic Stereotactic Body Radiation Therapy. *International Journal of Medical Physics, Clinical Engineering and Radiation Oncology*, **8**, 68-79.
https://doi.org/10.4236/ijmpcero.2019.82007

Received: February 19, 2019
Accepted: March 30, 2019
Published: April 2, 2019

Abstract

We investigated the feasibility of measuring daily fiducial length on cone-beam computed tomography (CBCT) images to assess the variation in daily tumor motion for pancreatic SBRT. Motion data for fifty pancreatic SBRT patients with fiducials were analyzed retrospectively to determine the tumor motion statistics. We also performed a phantom study which involved motion analysis of three gold fiducials placed around a solid target inside the Quasar Phantom as a function of variable tumor motion and breathing period. The end-exhalation CT-50 images were compared with the CBCT images acquired prior to treatment delivery on a TrueBeam STx linear accelerator. Sinusoidal tumor motion and patients' breathing files acquired from a Varian-RPM system were used to simulate patients' breathing patterns. The fiducial length was measured to determine its correlation with tumor motion. Patient tumor motions along the superior-inferior (SI), anterior-posterior (AP), and left-right (LR) directions were found to be 0.7 ± 0.4 cm, 0.2 ± 0.3 cm, and 0.1 ± 0.2 cm, respectively. Average breathing period was 4.3 ± 0.8 seconds. For sinusoidal and patients' breathing patterns, a significant correlation was observed between the fiducial length and tumor motions with R^2 of 0.99. However, fiducial length was found to be independent of the variation in breathing periods. This work suggests that measuring the fiducial length on daily CBCT images could provide quantitative daily tumor motion for fiducial-based pancreatic SBRT. A timely decision to modify the motion management strategy could be made prior to daily treatment delivery.

Keywords

Pancreas, SBRT, Fiducial, Tumor Motion, Inter-Fractional Tumor Motion

1. Introduction

Stereotactic Body Radiation Therapy (SBRT) of abdominal targets such as pancreatic and liver cancers has shown to be an effective treatment modality that could achieve high local control and reduced toxicity [1]-[6]. Although motion study provides insight on tumor motion during 4-dimensional (4D) Computed Tomography (CT) simulation, variations in inter- and intra-fractional target motion result in the loss of targeting accuracy and reproducibility compared to the original treatment plan [2] [7].

Several studies [7] [8] discussed the applicability of the motion study data acquired during 4D-CT simulation over the course of treatment delivery. Regarding the SBRT technique of abdominal targets, tumor motion over the treatment course is susceptible to the variability of abdominal filling, patient setup, and therapy/disease-related progression due to tight setup margins. Variations in daily tumor motion combined with suboptimal gating accuracy could introduce additional errors to the treatment delivery [8]. Therefore, it is important to evaluate the daily variation of tumor motion prior to beam delivery, and compare the daily tumor motion to the reference 4D-CT motion data in order to ensure the adequacy of the plan delivery.

Due to the limited tissue contrast on cone-beam CT (CBCT) images, it is not easy to determine the variation of tumor motion for pancreatic SBRT cases, which could result in dosimetric uncertainties. Therefore, gold fiducials are used for characterizing tumor motion during CT simulation as well as for target localization. These fiducials could also be used to evaluate the inter- and intra-fractional tumor motion.

In this study, we analyzed the tumor motion characteristics for pancreatic SBRT cases with gold fiducials. The feasibility of fiducial length-based tumor motion prediction was examined to evaluate the variation in daily tumor motion for pancreatic SBRT. Empirical correlation between tumor motion and fiducial length on CBCT images was investigated as a tool for the adjustment of the gating window on a daily basis.

2. Materials and Methods

2.1. Patient Characteristics for Pancreatic SBRT Cases

4D-CT data for 50 pancreatic SBRT patients were selected for this retrospective study. All patients had 2 - 3 gold fiducials (length of Visicoil = 5 mm) implanted inside the lesions or close to the lesions, and were treated using TrueBeam STx or Trilogy linear accelerator (Varian Medical Systems, Palo Alto, CA, USA). The prescription dose was 36 Gy in 3 fractions, and was delivered on an every other day schema. The prescribed isodose lines (IDL) for all cases were in the range of 80% - 90% of the target maximum dose.

2.2. Pancreatic SBRT Treatment Planning

In our clinic, pancreatic SBRT plan is generated using the Eclipse treatment

planning software (Varian Medical Systems, Palo Alto, CA, USA). A series of CT images of both 1.25 mm (*i.e.* helical free breathing scan) and 2.5 mm (axial 4D-CT scan) slice thickness are acquired for treatment planning purpose. Patient simulation is performed using a CT simulator (GE Health Care, Waukesha, WI, USA) with the BodyFix immobilization device (Elekta AB, Stockholm, Sweden). Varian Real-time Position Management (RPM^{TM}) is used to acquire 4D-CT images as well as to deliver the treatment plan. For coaching cases, monophasic respiratory coaching technique with "breathing in" sound enabled and "breathing out" sound disabled is implemented in order to minimize the hypo-ventilation issue during motion study. For tumors with motion of ≤ 5 mm in any direction, we use either helical free breathing CT or end-exhalation phase-50 CT images (CT-50) for treatment planning without any gating. On the other hand, for tumors with motion of >5 mm, we utilize the CT-50 images for treatment planning with gating.

On all treatment days, CBCT images are acquired and registered with the planning CT images. The superior border of the fiducial on the CBCT images is matched with the fiducial on the planning CT images. On the first day of treatment, we also confirm that the fiducial motion is within the 4D-CT motion data by using the fluoroscopic imaging.

2.3. Quasar Phantom Measurements

Three gold fiducials (length and width = 5 mm × 1 mm) were placed around the target insert supplied with the Quasar Phantom (Modus, London, Ontario, Canada). 4D-CT images were acquired with a tumor motion of 1 cm along the superior-inferior (SI) direction as shown in **Figure 1**. The breathing period was set to 4 seconds with a sinusoidal breathing pattern. After generating a 4D CT imaged, CT-50 images were imported into the Eclipse treatment planning system, and a set of setup fields were created for the acquisition of CBCT images.

Regarding the fiducial orientation, two different orientations were simulated; 90-degree angle, which is along the SI direction, and 45-degree angle compared to the SI direction. In our clinic, we did not observe any fiducials implanted with lateral or anterior-posterior directions, and hence we did not simulate any fiducials with zero or 180-degree angles.

CBCT images were acquired by using the half-fan pelvis technique in a TrueBeam STx linear accelerator. Sinusoidal tumor motion was simulated with a range of zero to 2 cm with 0.5 cm increment along the SI direction. For each tumor motion, the breathing period was varied from 2 to 6 seconds with 2 second increment.

In this study, patients' breathing files acquired using the Varian RPM system were used to simulate patients' breathing patterns. **Figure 2** shows an example of a patient's breathing file. After importing the VXP files, the waveform was inverted to simulate the correct breathing cycle in the Quasar Phantom. As the patient's breathing pattern was changed, the Quasar Phantom automatically adjusted the magnitude of tumor motion per the patient's breathing file. Due to the

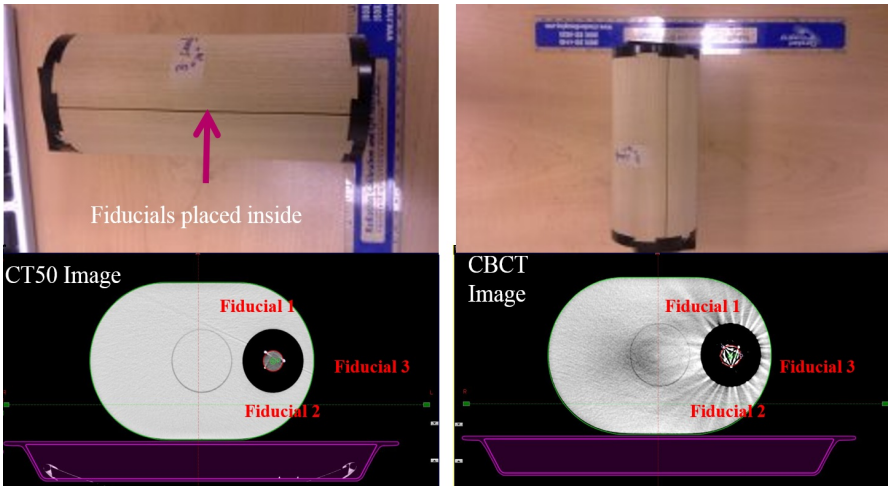

Figure 1. Quasar Phantom with three gold fiducials placed around the solid target insert. The image on the left shows an end-exhalation CT-50 image and the image on the right shows a CBCT image.

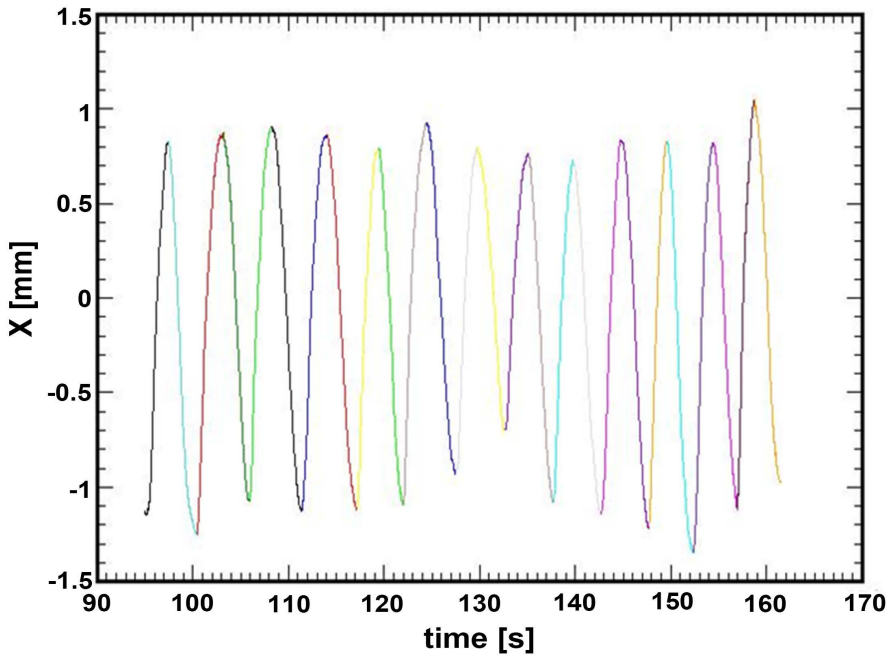

Figure 2. An example of a patient breathing waveform used to simulate tumor motion with the Quasar Phantom.

limitation of the Quasar Phantom, we set 2 mm as the magnitude of the patient waveform to mimic a non-moving case. Rotational motions of fiducials were not considered due to the one-dimensional (1D) characteristics of the Quasar Phantom.

With the window/level setting for abdomen in the Eclipse, the fiducial length on the CBCT images was determined by measuring the width of the Hounsfield unit (HU) profile, which is the width of the HU value of zero as shown in **Figure 3** in order to minimize any subjective bias. Measurement uncertainty was quantified

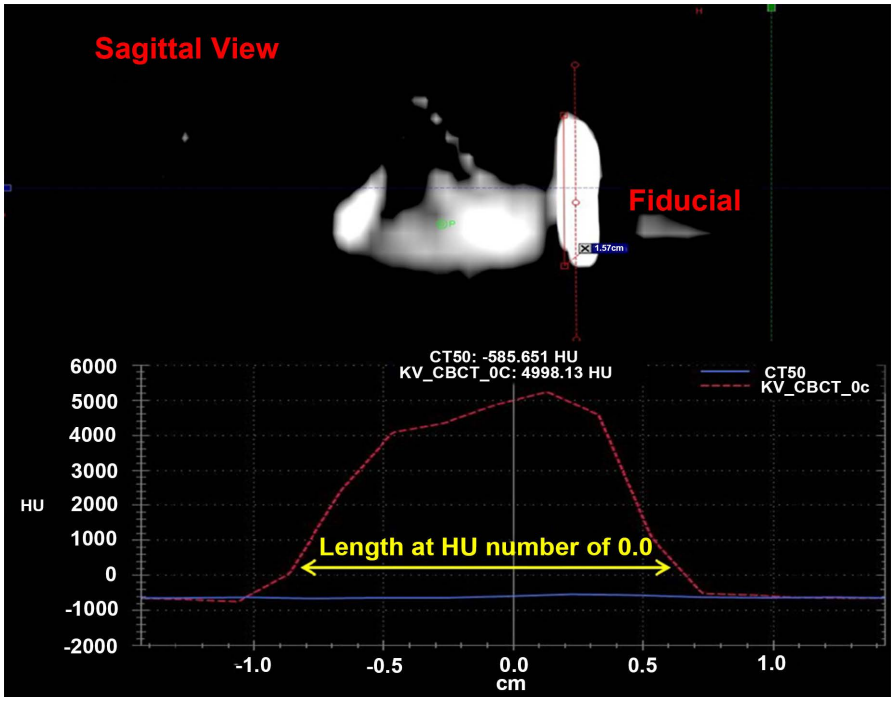

Figure 3. Quantification of gold fiducial length on the cone-beam CT image dataset by using the width of Hounsfield unit (HU) number of zero along the track of fiducial motion. Window/level setting for abdomen was used in the Eclipse treatment planning software.

by calculating the error bar of one standard deviation using the measured lengths of three gold fiducials.

3. Results

Fourteen patients were treated without gating technique because the tumor motion was ≤5 mm in any given direction. The mean breathing period was 4.3 ± 0.8 seconds (median = 4.0 seconds) with minimum and maximum periods of 2.5 seconds and 5.5 seconds. Based on the breathing period data of the 50 patients, the breathing cycle for the Quasar Phantom was varied from 2 to 6 seconds with 2 second increments. Mean tumor motions for SI, anterior-posterior (AP), and left-right (LR) directions were 0.7 ± 0.4 cm (median = 0.7 cm, maximum = 1.8 cm), 0.2 ± 0.3 cm (median = 0.0 cm, maximum = 0.7 cm), and 0.1 ± 0.2 cm (median = 0.0 cm, maximum = 1.0 cm), respectively. Sixty-four percent of the 50 patients had 4D-CT scans that were acquired using a monophasic coaching technique. Table 1 shows mean tumor motion along the SI direction for coaching versus no-coaching and gating versus non-gating. No-coaching cases show less tumor motion compared to coaching cases (mean tumor motion = 0.6 cm versus 0.8 cm along the SI direction). For gating cases only, the mean tumor motion along the SI direction was 0.9 ± 0.3 cm (median = 0.8 cm, maximum = 1.8 cm) compared to 0.4 ± 0.2 cm for the non-gating cases.

Figure 4(a) shows the mean fiducial length along the SI direction with varying tumor motion simulated by the Quasar Phantom. As the tumor motion

Table 1. Characteristics of fiducial motion along the superior-inferior direction for 50 pancreatic SBRT cases. Median motion was computed with the superior-inferior motion data set of the 50 SBRT cases, and maximum motion value was selected among the most superior-inferior motion data of the 50 SBRT cases.

	Superior-Inferior Motion (cm)	Median Superior-Inferior Motion (cm)	Maximum Superior-Inferior Motion (cm)
All Data	0.7 ± 0.4*	0.7	1.8
Coaching	0.8 ± 0.4	0.8	1.8
No Coaching	0.6 ± 0.3	0.6	1.0
Gating	0.9 ± 0.3	0.8	1.8
No Gating	0.4 ± 0.2	0.5	0.5

Note *: average ± 1 standard deviation.

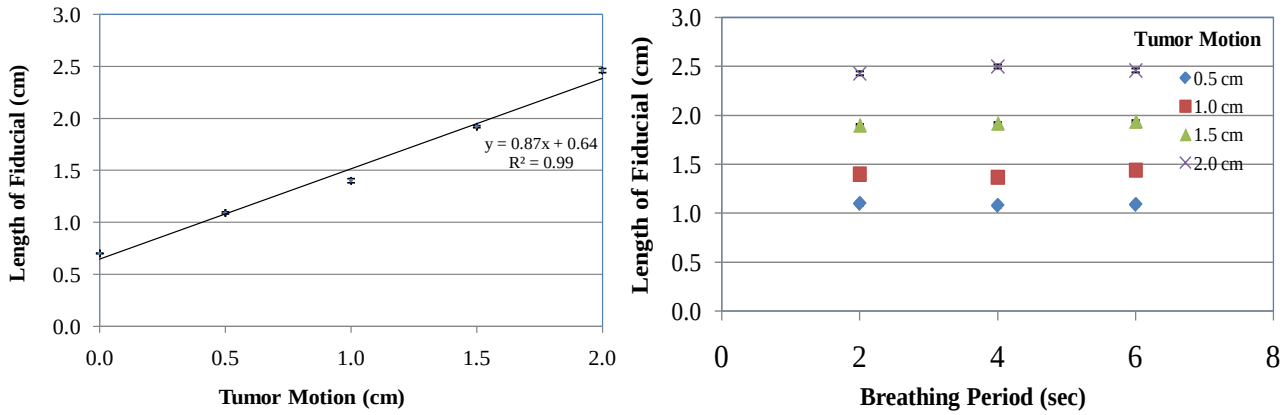

Figure 4. Variation of fiducial length for three fiducials along the superior-inferior direction as a function of tumor motion and breathing period, which was simulated by using the Quasar Phantom and sinusoidal breathing waveform. The error bar denotes one standard deviation calculated using the measured lengths of three fiducials. The magnitude of error bar was below 1 mm since all fiducials placed inside the Quasar Phantom were moved with the same characteristics of superior-inferior motion.

increased from no-motion to 2 cm, the mean fiducial length on the CBCT images increased linearly from 0.6 to 2.5 cm with a linear correlation of 0.87x + 0.64 cm ($R^2 = 0.99$). Figure 4(b) shows the mean fiducial length along the SI direction with varying breathing period of 2 seconds to 6 seconds. The mean fiducial length was independent of the breathing period regardless of the magnitude of tumor motion along the SI direction. Figure 5 shows how the mean fiducial length changes along the SI direction when the tumor motion increases from no-motion to 2 cm by using a breathing pattern that is representative of a patient's breathing pattern. Since the patient's breathing amplitude varied with time, the mean tumor motion increased from no-motion to 1.9 cm. The mean fiducial length was also found to increase linearly with varying tumor motion.

Table 2 shows the variation in length and width of three fiducials implanted at 45-degree angle along the SI direction as a function of tumor motion and breathing period of no motion, 2, 4, and 6 seconds, which measured with a

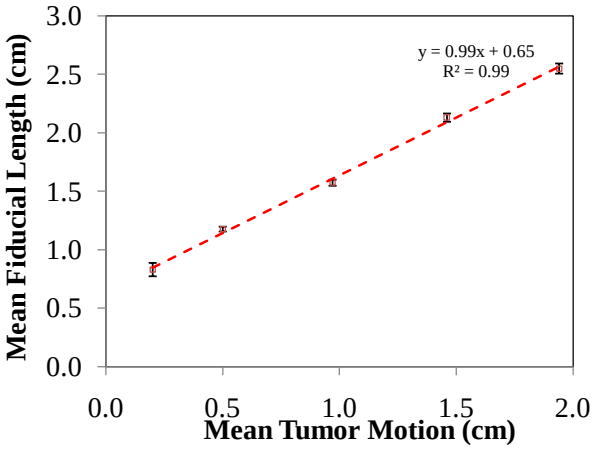

Figure 5. Variation of mean fiducial length for three gold fiducials implanted without fiducial rotation along the superior-inferior direction as a function of tumor motion, which was simulated by using a real patient's breathing waveform and the Quasar Phantom. The error bar denotes one standard deviation calculated using the fiducial lengths of three fiducials.

Table 2. Variations of three fiducials in length and width implanted at 45-degree angle along the superior-inferior direction as a function of tumor motion and breathing period of no motion, 2, 4, and 6 seconds, which was simulated by using the Quasar Phantom. The magnitude of error bar was below 1 mm since all fiducials placed inside the Quasar Phantom were moved with the same characteristics of superior-inferior motion.

Breathing Period (sec)	Tumor Motion (cm)	Fiducial Length (cm)	Fiducial Width (cm)
	No Motion	0.56 ± 0.00*	0.45 ± 0.04
	0.5	0.97 ± 0.05	0.45 ± 0.04
2	1.0	1.47 ± 0.05	0.45 ± 0.04
	1.5	1.90 ± 0.05	0.42 ± 0.05
	2.0	2.46 ± 0.03	0.39 ± 0.05
	No Motion	0.56 ± 0.00	0.45 ± 0.04
	0.5	0.97 ± 0.06	0.49 ± 0.03
4	1.0	1.41 ± 0.04	0.43 ± 0.06
	1.5	1.83 ± 0.01	0.43 ± 0.03
	2.0	2.44 ± 0.02	0.35 ± 0.07
	No Motion	0.56 ± 0.00	0.45 ± 0.04
	0.5	1.02 ± 0.03	0.51 ± 0.02
6	1.0	1.45 ± 0.03	0.45 ± 0.06
	1.5	1.83 ± 0.05	0.42 ± 0.03
	2.0	2.47 ± 0.03	0.36 ± 0.06

Note: * = average ± 1 standard deviation.

patient's breathing waveform. The mean fiducial length increased linearly with varying tumor motion.

4. Discussion

It is now well-established that the effectiveness of abdominal SBRT is affected by organ motion and the uncertainty of target positioning due to breathing motion [3]. At our institution, we use the end-exhalation CT-50 image for pancreatic SBRT planning because end-expiration phase shows the least target position variability, thereby allowing us to reduce the margin that is used for the internal target volume (ITV) definition [3] [9].

This study shows that the dominant tumor motion is along the SI direction (median SI motion of 0.7 cm versus median motion of 0 cm along the AP and LR directions) as reported in the literature [10] [11]. However, the magnitude of tumor motion in this study is different from data presented by Huguet *et al.* [10] and Langen *et al.* [11], which data show a mean motion of 1.8 - 2.0 cm and 1.3 cm along the SI direction, respectively. The difference in tumor motion along the SI direction between this study and Hugget *et al.* could be related to the immobilization device (BodyFix in our clinic versus Alpha Cradle in their clinic). Wunderink *et al.* also reported that abdominal compression for liver SBRT reduced the median liver tumor excursion by 62% along the SI direction [12].

AAPM TG-76 states that the magnitude of respiration-induced tumor motion might change (either increase or decrease) during the course of radiation treatment [13]. Nelson *et al.* reported a large inter-fractional variation in gated and non-gated fiducial motion for lung cases [14]. Using fluoroscopic studies, Ge *et al.* showed that the gating accuracy decreased by up to 50% for abdominal tumors. They attributed this decrease to the changes in external-internal correlation over time, suboptimal gating setup, and imperfections in the external-internal correlation [8]. They suggest that the inter-fractional variation of tumor motion for hypo-fractionated pancreatic SBRT should be assessed by using fluoroscopy or other tools before each treatment. However, there are presently no tools available to perform a quantitative evaluation of pancreatic tumor motion during treatment delivery. Although 4D-CBCT technology is currently available, there is no clinically relevant solution to analyze abdominal 4D-CBCT images prior to treatment since the quality of abdominal CBCT images is suboptimal. Fluoroscopy serves as an option to evaluate the daily fiducial motion. However, it provides mostly qualitative information about the fiducial motion.

Gierga *et al.* reported that treatment margins for abdominal tumors should be determined based on a detailed analysis of tumor motion rather than relying on the external-marker information [15]. Although a planning target volume (PTV) expansion of 2 - 5 mm is typically considered for pancreatic SBRT to account for setup uncertainty, strategies for motion management should be implemented to minimize PTV expansion [16]. In the present study, our goal was to determine whether daily variation of fiducial length on CBCT images could be used as a

tool to quantify the variability of daily tumor motion for pancreatic SBRT. Our results show that the measured fiducial length increased linearly from 0.7 cm to 2.5 cm for the simulated tumor motion of no-motion to 2 cm. Since the measured fiducial length has a strong correlation with tumor motion, it is possible to establish a correlation between the fiducial length on the CBCT images and tumor motion for pancreatic SBRT. Therefore, the variation in daily tumor motion could be determined by measuring the fiducial length on daily CBCT images.

Our approach assumes that the intra-fractional motion remains similar to the motion observed from the CBCT. In this study, we first investigated the feasibility of fiducial length-based motion prediction by using fixed magnitude of motion and breathing cycle, which excluded any impact of intra-fractional motion. Secondly, we used real patients' breathing files, which had irregular breathing patterns, in order to evaluate the combined effects of intra- and inter-fractional motions. For both measurements, there were consistent correlations between tumor motion and fiducial length on CBCT images with R^2 of 0.99. However, more precise quantification of the intra-fractional fiducial motion during treatment could only be achieved if real-time images are taken during delivery.

If the fiducial length-based motion exceeds the expected tumor motion from the 4D-CT motion study, it should be an indication to investigate whether the gating window should be adjusted or whether we need to work with the patient to minimize any deep-breathing that could cause an unexpected increase in tumor motion. Coaching cases show more tumor motion compared to no-coaching cases (mean tumor motion = 0.6 cm for no-coaching versus 0.8 cm for coaching along the SI direction) as shown in Table 1. If the fiducial length-based tumor motion exceeds the baseline motion data, respiratory guidance could be switched from coaching into no-coaching to reduce tumor motion. Additionally, fluoroscopic imaging without coaching could be implemented to make sure that the fiducial motion is within the expected motion from the motion study.

In real pancreatic SBRT cases, fiducial orientation is oblique rather than 90-degree angle, which is along the SI direction. In this study, fiducial length was measured with two different orientations of 90-degree and 45-degree. With different fiducial orientations, the mean fiducial length increased linearly with varying tumor motion, showing that fiducial-based motion measurement is less sensitive to the fiducial orientation.

A limitation of the present study is the uncertainty of the fiducial length measurement on the CBCT images with relatively short inspiration duration compared to the exhalation period. For an extremely short inspiration duration, the inferior tail of the gold fiducials shows lower HU numbers along the track of the fiducial motion compared to the superior boarder of gold fiducials. This smearing effect could result in a higher uncertainty in fiducial length measurements. In this study, measurement uncertainty represented by the error bar of one standard deviation was not great, which results from the fiducials implanted closely around the target in our attempt to mimic a real pancreatic SBRT case.

Additionally, this was a phantom study and all fiducials were moved with the same magnitude of motion and breathing cycle. All of the controlled motion measurements contributed to the minimal deviation of fiducial motions among the three fiducials. In our clinic, gold fiducials for pancreatic SBRT are usually implanted within 1 - 3 centimeters along the SI direction, and hence the motion characteristics of individual fiducial should have a similar pattern as shown in this study.

Rotational motion was not considered in this study, which was a limitation of this study. The 1D breathing data acquired for real patients do not represent the three-dimensional (3D) motion characteristics, which could be not only translational but also rotational. Therefore, the measured fiducial length might be varied through the breathing cycle. However, this study showed that the dominant motion of pancreatic tumors was along the SI direction (median SI motion of 0.7 cm versus median motion of 0 cm along the AP and LR directions). Regarding rotational motion, Xu *et al.* [17] reported that the rotational angles in roll, pitch, and yaw for CyberKnife-based liver SBRT were 1.2˚ ± 1.8˚, 1.8˚ ± 2.4˚, and 1.7˚ ± 2.1˚, respectively. Bertholet *et al.* [18] also showed that the mean intrafractional rotations for fiducials were 3.9˚ (LR), 2.9˚ (SI), and 4.0˚ (AP) for liver SBRT, which was evaluated using the projection images of CBCT scans. Considering the dominant SI translational motion in pancreatic SBRT cases as well as small rotational motions of less than 4˚, the estimation of daily tumor motion using fiducial length measurements could be a feasible option in a clinical setting.

5. Conclusion

For pancreatic SBRT, the measured fiducial length on the CBCT images correlates well with the magnitude of tumor motion observed in the phantom study. Our results show that daily tumor motion could be evaluated by measuring the fiducial lengths on daily CBCT images. A decision as to whether the motion management techniques are to be modified for that particular day (e.g. change the gating window, etc.) could be made in a timely manner.

Conflicts of Interest

The authors declare no conflicts of interest regarding the publication of this paper.

References

[1] Yang, W., Fraass, B.A., Reznik, R., *et al.* (2014) Adequacy of Inhale/Exhale Breath-Hold CT Based ITV Margins and Image-Guided Registration for Free-Breathing Pancreas and Liver SBRT. *Radiation Oncology*, **9**, 11. https://doi.org/10.1186/1748-717X-9-11

[2] Goyal, K., Einstein, D., Ibarra, R., *et al.* (2012) Stereotactic Body Radiation Therapy for Nonresectable Tumors of the Pancreas. *Journal of Surgical Research*, **174**, 319-325. https://doi.org/10.1016/j.jss.2011.07.044

[3] Katz, A.W., Carey-Sampson, M., Muhs, A., *et al.* (2007) Hypofractionated Stereotactic Body Radiation Therapy (SBRT) for Limited Hepatic Metastases. *International Journal of Radiation Oncology Biology Physics*, **67**, 793-798. https://doi.org/10.1016/j.ijrobp.2006.10.025

[4] Chuong, M.D., Springett, G.M., Freilich, J.M., *et al.* (2013) Stereotactic Body Radiation Therapy for Locally Advanced and Borderline Resectable Pancreatic Cancer Is Effective and Well Tolerated. *International Journal of Radiation Oncology Biology Physics*, **86**, 516-522. https://doi.org/10.1016/j.ijrobp.2013.02.022

[5] Rwigena, J.C., Parikh, S.D., Heron, D.E., *et al.* (2011) Stereotactic Body Radiotherapy in the Treatment of Advanced Adenocarcinoma of the Pancreas. *American Journal of Clinical Oncology*, **34**, 63-69. https://doi.org/10.1097/COC.0b013e3181d270b4

[6] Stauder, M. and Miller, R.C. (2010) Stereotactic Body Radiation Therapy (SBRT) for Unresectable Pancreatic Carcinoma. *Cancers*, **2**, 1565-1575. https://doi.org/10.3390/cancers2031565

[7] Michalski, D., Sontag, M., Li, F., *et al.* (2008) Four-Dimensional Computed Tomography-Based Interfractional Reproducibility Study of Lung Tumor Intrafractional Motion. *International Journal of Radiation Oncology Biology Physics*, **71**, 714-724. https://doi.org/10.1016/j.ijrobp.2007.10.038

[8] Ge, J., Santanam, L., Yang, D. and Parikh, P.J. (2013) Accuracy and Consistency of Respiratory Gating in Abdominal Cancer Patients. *International Journal of Radiation Oncology Biology Physics*, **85**, 854-861. https://doi.org/10.1016/j.ijrobp.2012.05.006

[9] O'Dell, W.G., Schell, M.C., Reynolds, D. and Okunieffm, P. (2002) Broadening Due to Target Position Variability during Fractionated Breath-Held Radiation Therapy. *American Association of Physicists in Medicine*, **29**, 1430-1437. https://doi.org/10.1118/1.1485977

[10] Huguet, F., Yorke, E., Davidson, M., *et al.* (2015) Modeling Pancreatic Tumor Motion Using 4-Dimensional Computed Tomography and Surrogate Markers. *International Journal of Radiation Oncology Biology Physics*, **91**, 579-587. https://doi.org/10.1016/j.ijrobp.2014.10.058

[11] Langen, K.M. and Jones, D.T.L. (2001) Organ Motion and Its Management. *International Journal of Radiation Oncology Biology Physics*, **50**, 265-278. https://doi.org/10.1016/S0360-3016(01)01453-5

[12] Wunderink, W., Romero, A.M., Kruuf, W.D., *et al.* (2008) Reduction of Respiratory Liver Tumor Motion by Abdominal Compression in Stereotactic Body Frame, Analyzed by Tracking Fiducial Markers Implanted in Liver. *International Journal of Radiation Oncology Biology Physics*, **71**, 907-915. https://doi.org/10.1016/j.ijrobp.2008.03.010

[13] Keall, P.J., Mageras, G.S., Balter, J.M., *et al.* (2006) The Management of Respiratory Motion in Radiation Oncology Report of AAPM Task Group 76. *Medical Physics*, **33**, 3874-3900. https://doi.org/10.1118/1.2349696

[14] Nelson, C., Starkschall, G., Balter, P., *et al.* (2006) Assessment of Lung Tumor Motion and Setup Uncertainties Using Implanted Fiducials. *International Journal of Radiation Oncology Biology Physics*, **67**, 915-923. https://doi.org/10.1016/j.ijrobp.2006.10.033

[15] Gierga, D.P., Brewer, J., Shart, G.C., *et al.* (2004) The Correlation between Internal and External Markers for Abdominal Tumors: Implications for Respiratory Gating. *International Journal of Radiation Oncology Biology Physics*, **61**, 1551-1558.

[16] Trakul, N., Koong, A.C. and Chang, D. (2014) Stereotactic Body Radiotherapy in the Treatment of Pancreatic Cancer. *Seminars in Radiation Oncology*, **24**, 140-147. https://doi.org/10.1016/j.semradonc.2013.11.008

[17] Xu, Q., Hanna, G., Grimm, J., *et al.* (2014) Quantifying Rigid and Nonrigid Motion of Liver Tumors During Stereotactic Body Radiation Therapy. *International Journal of Radiation Oncology Biology Physics*, **90**, 94-101. https://doi.org/10.1016/j.ijrobp.2014.05.007

[18] Bertholet, J., Worm, E.S., Fledelius, W., *et al.* (2016) Time-Resolved Intrafraction Target Translations and Rotations during Stereotactic Liver Radiation Therapy: Implications for Marker-Based Localization Accuracy. *International Journal of Radiation Oncology Biology Physics*, **95**, 802-809. https://doi.org/10.1016/j.ijrobp.2016.01.033